Controller Robustness Analysis of Grid-tied AC-stacked PV Inverter System Considering Manufacturing Inaccuracies

Hamidreza Jafarian, Mehrdad Biglarbegian, Babak Parkhideh
Electrical and Computer Engineering Department
Energy Production and Infrastructure Center (EPIC)
University of North Carolina at Charlotte
Charlotte, NC, USA
{hjafaria, mbiglarb, bparkhideh}@uncc.edu

***Abstract*— This paper analyzes the impact of current sensing inaccuracies due to aging and ambient condition variations on robust operation of PV inverter systems. A novel index for analyzing the robustness of grid-tied AC-stacked PV inverter architectures has been used, which provides an opportunity for comprehensive robustness evaluation by considering four major operational characteristics of grid-tied PV inverters as efficiency, Total Harmonic Distortion (THD), Power Factor (PF) compliance, and Maximum Power Point Tracking (MPPT) effectiveness. In addition, a comparative analysis between a single inverter and an AC-stacked inverter configuration is provided to study the impact of AC-stacking on robust operation of grid-tied PV inverters. This paper also proposes a possible state estimation solution for improving the robustness of the system using Kalman filter approach.**

Keywords—Grid-tied PV Inverter, AC-stacked PV Inverter, Reliability, Robustness, Karlman Filter, Smart Inverter Robustness Index, Current Sensing Inaccuracy.

I. INTRODUCTION

Recent years, the advent of new power electronics technologies and dramatic cost reduction of Photovoltaic (PV) modules have led to a significant increase in solar PV system capacities in both distribution and transmission power system networks [1, 2]. In power networks with high penetration of PV systems, efficient and reliable operation of the system depends on robust operation of the inverter system. Therefore, reliability and robustness of inverters should be considered and examined during the design and operation of power system networks [3, 4]. Reliability-based design of grid-tied PV inverters was initially proposed in 2015 [5]. To provide comprehensive analysis of grid-tied PV inverter's robustness, there are multiple parameters that should to be considered and can be categorized as: efficiency, Total Harmonic Distortion (THD), power factor (PF) compliance, Maximum Power Point Tracking (MPPT) accuracy.

Among all of these factors, conversion efficiency has the highest impact on reliability and robust operation of PV inverters, which have been analyzed in [6] from the topology and control point of view. Efficiency analysis of different PV inverter topologies and different semiconductor devices have been presented recently. The impact of control architecture on efficiency of low switching frequency PV inverter topologies as well as the impact of physical variations of the main components of PV inverters on conversion efficiency were studied in [7-9]. The inverter performance metrics such as efficiency not only depend on topology and control scheme, but they also depend on the characteristics of employed components such as passive and sensing elements [10]. Characteristics of sensing components, particularly current sensors can be varied based on different parameters such as manufacturing inaccuracies and ambient condition changes like temperature, humidity, and aging. The impact of physical variations of these components in efficiency of PV inverters has been analyzed in the recent published studies [7, 11, 12].

The second important parameter for robustness evaluation of inverters is THD. The semiconductors used in the power electronics' converters, inject harmonic distortion into power networks. Therefore, this parameter directly could mitigate robustness of the system, due to power quality and standard restrictions. The problem may become sever by increasing the number of PV inverters in the future grids. In recent years, several research focused on attenuating the harmonic distortion of grid connected PV inverters output current [13-16]. The third parameter is PF compliance. Since a reliable operation of power networks with high penetrated PV systems is dependent on ancillary services from distributed generations such as reactive power support, PF correction plays a crucial role in grid-tied PV inverters [17-19]. Finally, MPPT accuracy also impacts on the robust operation of grid-tied PV inverters. MPPT accuracy is highly dependent on ambient condition changes, and component inaccuracies that may directly affect the robustness of PV inverter systems [20, 21].

This paper utilizes the Smart Inverter Robustness Index (SIRI), which was initially introduced in 2016 [12]. This new performance metric was proposed to evaluate the robustness of grid-tied PV inverter systems considering four major performance characteristics presented above. This paper aims to

analyze the impact of sensing inaccuracies due to aging and ambient condition changes (temperature) on the robust operation of grid-tied PV inverters and represent them based on SIRI index. Section II presents the SIRI in detail and statistical analysis for obtaining this parameter according to system model. In section III, two grid-tied PV inverter architectures are provided and a Kalman filter estimation algorithm is added to the system to estimate the output current. The outcome of the estimation can be used to compensate inaccuracies of the sensing devices, which results in improvement of system robustness in grid-tied inverters. The impacts of cascading the inverters on the robust operation of both generic grid tied PV inverter and an AC-stacked PV inverter will be compared in section IV. Finally, conclusion and remarking notes are provided in section V.

II. SMART INVERTER ROBUSTNESS ANALYSIS

PV inverter operation and lifetime are highly dependent on performance of electrical components. One of the most important electrical components in modern PV inverters with distributed architecture and high frequency switching is a current sensing device. The performance of different current sensor technologies such as hall-effect, magneto resistor-based, and fluxgate current sensors with wide band of operational characteristics highly rely on manufacturing accuracy, variations of environmental conditions and changes in component's characteristics due to aging. Therefore, reliability and robustness of PV inverters will be affected respectively. Since physical variations is a consequence of the inherent randomness in electrical components, in order to analyze the impact of these uncertainties on performance of PV inverters, the system should be statistically analyzed. Different statistical analysis methods can be used for solving this problem, but as the most favorite one is Monte Carlo Sampling method. This method utilizes statistical analysis and random sampling experiments to provide approximate solutions for unformulated problems, which are random in nature and it is very difficult to solve [22]. Monte Carlo statistical analysis was utilized in the semiconductor industry to prove the feasibility of manufacturing of systems consisting several semiconductor devices. Similar approaches are expected to arrive when several components and devices work cooperatively together in a system such as PV inverters. Therefore, Monte Carlo method is widely applied for reliability and robustness analysis of PV inverters [12].

Monte Carlo analysis requires a large number of sampling points for solving big statistical problems with several uncertain variables. By using variance reduction techniques, the required number of sampling points can be reduced and consequently the simulation time reduced significantly. A commonly used variance reduction method known as the Latin Hypercube Sampling (LHS) is a type of stratified Monte Carlo sampling algorithms, which used in this paper. The LHS method not only reduces the required number of sampling points, but also improves the accuracy and confidence in the results. In this method, cumulative distribution function is divided into few equally probable sub-sections and the equal number of sampling points are selected from these sub-sections. Therefore, this method by spreading sampling points can reduce the required points significantly [23, 24]. In this paper, Random Latin Hypercube Sampling (RLHS) algorithm is used to model the impact of uncertainties of current sensing devices with minimum sampling points. Current sensor variations is modeled by a random scaling factor, which multiplied to sensor measurements and a random offset value is also added to the measurements. Robustness evaluation depends on an index named Smart Inverter Robustness Index (SIRI) [12], which quantifies the robust operation of PV inverters. In this parameter, conversion efficiency, THD, PF, and MPPT are all contrived to present the main operational characteristics of grid connected PV inverters in this index. SIRI consists of these operation characteristics is shown in (1).

In this index, for each performance characteristic a limitation factor is defined. For conversion efficiency, PF, MPPT effectiveness, the limitating factor is the minimum acceptable value that can be described according to application and standards. Also, for the THD term, the maximum acceptable value is defined based on IEEE standard 519-1992, which is 5%. The minimum acceptable conversion efficiency for this generic grid-tied PV inverter and AC-stacked PV inverter is 95%, and this value can be different based on application and configurations. In this paper, the limit for PF compliance and MPPT effectiveness is defined as 99%.

By analyzing the system based on selected sampling points, if all the four terms in the SIRI are positive, this would mean the inverter is in robust region. On the other hand, if one of the normalized terms is negative, the inverter operates outside of the robustness region and the SIRI will be highlighted as -1. Therefore, a relative index can be developed to comparatively evaluate the inverter robustness operation in different regions. In this index, each term is appropriately normalized to the maximum acceptable error, which means the higher values in SIRI, the more robust is the PV inverter operation.

$$SIRI = \begin{cases} \dfrac{(PF - k_{pf})}{(1-k_{pf})} \times \dfrac{(Eff - k_{Eff})}{(1-k_{Eff})} \times \dfrac{((1-THD)-(1-k_{THD}))}{k_{THD}} \times \dfrac{(MPPT_{Eff} - k_{MPPT})}{(1-k_{MPPT})}, \\ \qquad PF > k_{pf}, Eff > k_{Eff}, THD < k_{THD} or MPPT_{Eff} > k_{MPPT} \\ -1, \qquad PF < k_{pf}, Eff < k_{Eff}, THD > k_{THD} or MPPT_{Eff} < k_{MPPT} \end{cases} \tag{1}$$

where:

k_{pf}	The minimum acceptable Power Factor compliance accuracy	k_{THD}	The maximum acceptable THD
k_{Eff}	The minimum acceptable Conversion Efficiency	k_{MPPT}	The minimum acceptable MPPT effectiveness

III. GRID-TIED PV INVERTER

A. Single Inverter

The impact of current sensing inaccuracies on a single gird-tied PV inverter will be analyzed in the next section. Control scheme of the single grid-tied PV inverter consists of two cascaded control loops shown in Fig. 1. As it can be observed here, different inaccuracies are existed in sensing elements or passive components that could have an impact on the operation of the PV inverter. The focus of this paper will only be on current sensing inaccuracies, which is highlighted as black in the figure.

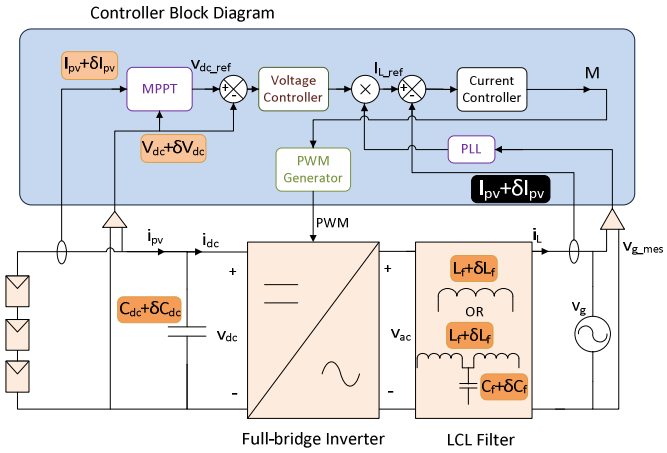

Fig. 1. Single inverter schematic and control block diagram.

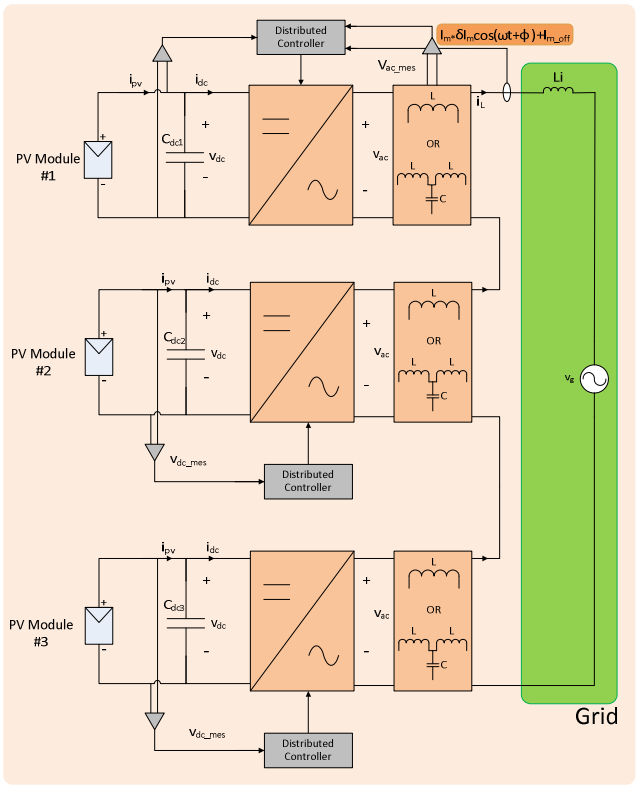

Fig. 2. Grid-tied AC-stacked PV inverter architecture with current sensing inaccuracies.

B. AC-stacked PV Inverter

By analyzing a single grid-tied inverter system and AC-stacked PV inverter system, the impact of cascading inverters on the robustness of AC-stacked PV inverter system will be evaluated [24] in the following section. This architecture consists of three module-level inverters connected to the grid. The power level of this system is equal to the single inverter system presented in the previous section. In this system, a perturb and observe algorithm is used for Maximum Power Point Tracking (MPPT) of inverters. Each inverter has a DC-bus voltage controller that regulates its own voltage based on the output of MPPT stage. In this architecture, one inverter is responsible to control the current of the whole PV string system. This inverter has a current sensor, which might have inaccuracy due to aging and environmental conditions. These inaccuracies affect the current measurement output by a scale factor, offset factor, and phase shift factor as shown in Fig. 2.

C. Modelling and State Estimation

To prescribe the system more accurately, the nonlinear state space model of AC-stacked inverter system is presented in (2).

$$\begin{cases} \dfrac{dV_{dc1}}{dt} = \dfrac{I_{PV1}}{C_{dc1}} - \dfrac{I_d m_{d1}}{C_{dc1}} - \dfrac{I_q m_{q1}}{C_{dc1}} \\ \dfrac{dV_{dc2}}{dt} = \dfrac{I_{PV2}}{C_{dc2}} - \dfrac{I_d m_{d2}}{C_{dc2}} - \dfrac{I_q m_{q2}}{C_{dc2}} \\ \dfrac{dV_{dc3}}{dt} = \dfrac{I_{PV3}}{C_{dc3}} - \dfrac{I_d m_{d3}}{C_{dc3}} - \dfrac{I_q m_{q3}}{C_{dc3}} \\ \dfrac{dI_d}{dt} = -\dfrac{V_{dc1} m_{d1}}{L_g} - \dfrac{V_{dc2} m_{d2}}{L_g} - \dfrac{V_{dc3} m_{d3}}{L_g} - \omega I_q + \left(\dfrac{V_g}{L_g}\right) \\ \dfrac{dI_q}{dt} = -\dfrac{V_{dc1} m_{d1}}{L_g} - \dfrac{V_{dc2} m_{d2}}{L_g} - \dfrac{V_{dc3} m_{d3}}{L_g} + \omega I_d \end{cases} \quad (2)$$

where:

$C_{dc1}, C_{dc2}, C_{dc3}$	DC-link capacitors *(F)*
$I_{PV1}, I_{PV2}, I_{PV3}$	PV modules output current *(A)*
L_g	Grid inductance *(H)*
V_g	Grid voltage *(V)*
ω	Frequency $\left(\frac{rad}{s}\right)$
$V_{dc1}, V_{dc2}, V_{dc3}$	DC voltages input of individual inverters *(V)*
m_{d1}, m_{d2}, m_{d3}	d-component of modulation indices
m_{q1}, m_{q2}, m_{q3}	q-component of modulation indices
I_d	d-component of output current injected to the grid *(A)*
I_q	q-component of output current injected to the grid *(A)*

Provided the state space equations of the AC-stacked PV inverters shown in (2), the Kalman filter algorithm can be employed to estimate the system parameters with limited measurements and speed up the response after disturbances. In this architecture, for the estimation of the current sensor

output, which represents the inductor current, the Kalman filter is essentially being running an algorithm with the proposed model and calculated the residual differences. Fig. 3 shows how the parameters for Kalman Filter are being formulated. While the algorithm is running, the convergence of developed system should be reached to constant value provided by measurements and system process. Fig. 3 shows how these recursive formulas need to be updated to achieve the proper output estimation [25].

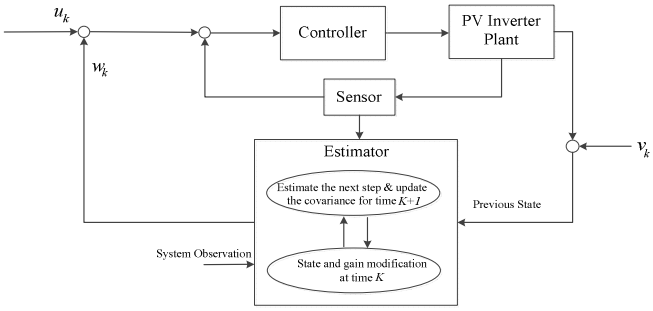

Fig. 3. Proposed scheme for modeling and system estimation

$$\hat{x}_{k+1|k} = A_{k+1}\hat{x}_{k|k} + v_{k+1} \tag{3}$$

$$P_{k+1|k} = A_{k+1}P_{k|k}A_{k+1}^{T} + Q_{k+1} \tag{4}$$

$$z_k = C_k\hat{x} + R_k \tag{5}$$

As shown in (3), $\hat{x}$ is the estimation space vector that represents the state transition of the model. The propagator matrix A_k shows the estimation of the state in the next time interval as $k+1$. Furthermore, the covariance matrix of the state estimation is called P_k. Q_k is a normalized covariance matrix of sensor noise introduced by v_k. In equation (4), R_k is a normalized covariance matrix of the measurement error and state transitions should be updated according to:

$$\hat{x}_{k|k} = \hat{x}_{k|k-1} + K_k(z_k - C_k\hat{x}_{k|k}) \tag{6}$$

$$K_k = P_{k|k-1}C_k^{T}(C_kP_{k|k-1}C_k^{T} + R_k^{T})^{-1} \tag{7}$$

$$P_{k|k} = (1 - K_kC_k)P_{k|k-1} \tag{8}$$

where K_k shows the Kalman filter gain and in (8), the updated covariance matrix will be assigned to the (4). As it can be observed, the measurements have been connected to state transitions linearly. Since the primary purpose of this estimation is to minimize the effect of observation noise, therefore the process noise was considered static during running the algorithm operation.

The current sensor accuracy and its limitation typically has been discussed in articles as bandwidth limitations, temperature drift, DC current saturation, hysteresis saturation. Assuming operating the converter at safe area which will not be affected by these physical limitations, there are some other concerns that the sensor characteristics can be engaged. The ambient variations such as temperature and humidity can change current sensor characteristics and it evolves as inaccuracy. For instance, for most of Hall-Effect based current sensors zero current offset inaccuracy, sensitivity changes, and nonlinearity variations of the sensor respect to temperature have been reported. There are some other parameter changes such as magnetic nonlinearity, or magnetic noise spectrum interferences for magneto-resistive-based current sensors. Lack of internal voltage references for flux gate sensors, or magnetic sensitivity in Rogowski-based current sensors are the most important limitations in these sensors [8], [26].

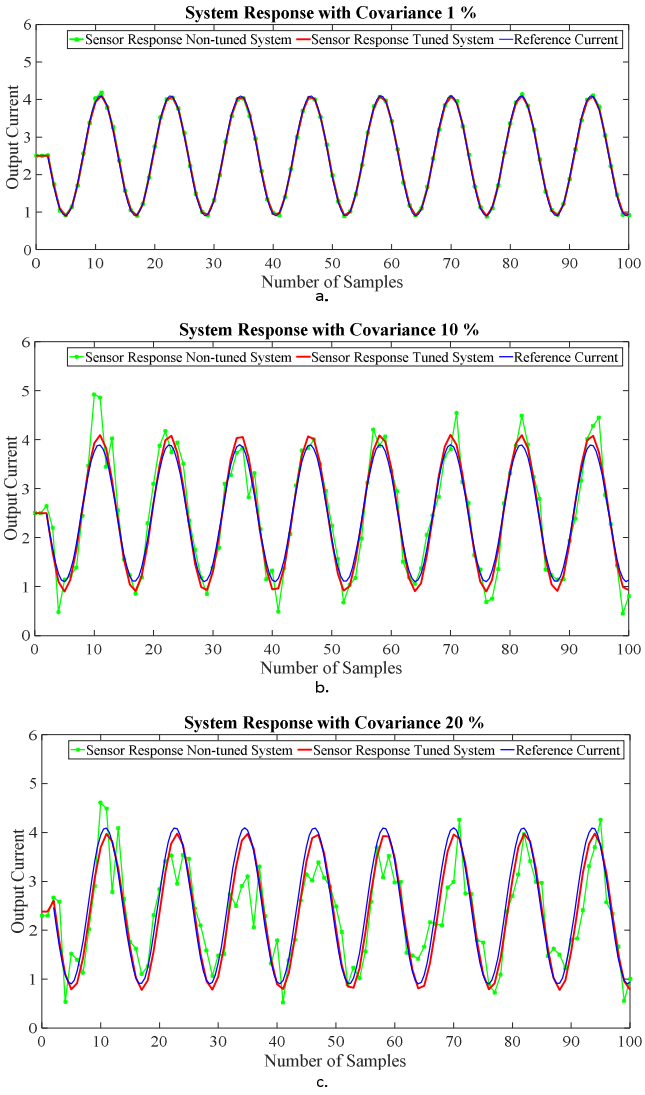

Fig. 4. The current sensor response under three different conditions with different covariance error. Blue: ideal waveform, Green: actual system reference response, Red: modified system response correction with Kalman filter estimation. a. 1% covariance error in current sensor response, b. 10% covariance error in current sensor response. c. 20% covariance error in current sensor response.

Since in the hardware setup, the Hall-effect current sensor (ACS714/ACS730 from Allegro) has been used, three different parameters of zero current offset inaccuracy, sensitivity changes, and nonlinearity variations of the sensor

respect to temperature were considered [27, 28]. The absolute error variations of the sensor is represented as:

$$E_{abs} = \overline{E_{offset}} \times \overline{E_{sensitivity}} \times \overline{E_{non\_linearity}} \quad (9)$$

where, E_{offset}, $E_{sensitivity}$ and $E_{non\_linearity}$ are random zero current offset changes, sensitivity, and nonlinearity variations respectively, versus temperature based on manufacturer datasheet. Therefore, the normalized covariance matrix of measurement error has been established accordingly. Since the PV inverters are going to be used during the days where the temperature is higher, this study focuses on the sensor measurement estimation in the temperature range of 20-45℃. This means the normalized covariance measurement matrix can be formulated more accurately in this temperature range. Thus, the system response error modification depending on the accuracy of temperature variations of the sensor can be modeled and normalized, respectively. In the next step, the updated observable matrix by applying filter gain, can be replaced with the measurement absolute value.

Fig. 4 shows the current sensor response in three different scenarios with minor, moderate, and major covariance errors. The overall system response with respect to current sensor output can be modified through the Kalman filter algorithm. As it can be observed in Fig. 4, while the plant observes the higher covariance sensor noise, the modified estimation has more error respect to ideal waveform.

IV. Results

In order to analyze the impact of AC stacking on robust operation of PV system, two MATALB Simulink models are built based on schematics and control schemes shown in Fig. 1 and Fig. 2.

TABLE I. performance characteristics and SIRI index values for single gird-tied PV inverter system with different current sensing inaccuracies

Standard Deviation	Efficiency	Power Factor	THD	MPPT	SIRI
0%	98.23%	0.9996	1.3%	99.93%	0.4282
1%	97.13%	0.9997	1.37%	99.65%	0.1211
5%	96.9%	0.9994	1.4%	99.56%	0.096
7%	96.37%	0.9993	1.6%	99.12%	0.0237
8%	96.09%	0.9992	1.6%	98.95%	-1

Since robustness analysis is a statistical analysis and requires several operating conditions, it is not practical to perform the analysis on hardware setup. Therefore, simulation models verified by hardware test-beds in nominal operating point and statistical analysis is also performed on the verified simulation model. In an individual PV inverter system, the input voltage of the inverter is stabilized by a DC capacitor. The inverter switches at 40kHz and output voltage is filtered out by an LC filter. TABLE I presents the impact of increasing current sensing inaccuracies on robust operation of a single grid-tied PV inverter. As it can be seen in this table, increasing inaccuracies will reduce MPPT precision, and system efficiency. This system operates in robust region till 7% standard deviation, which is the boundary of robustness. For the inaccuracies more than 7%, the system enters in un-robust region where SIRI sets on -1. Fig. 5 shows how increasing current sensing inaccuracies reduces the system robustness, which is represented by SIRI. Comparing Fig. 5 and Fig. 6, it can be concluded that by cascading the PV inverters and using a decentralized control approach, boundary of robustness is increased to 17% standard deviation. This happens because the current sensing inaccuracy has a direct impact on the MPPT accuracy of the PV inverter system. However, in AC-stacked architecture, *(n-1)* have been controlled by DC-bus voltage control and their MPPT operations are not affected by current sensing inaccuracies. Therefore, MPPT accuracy of whole structure could raise up and make the system more robust.

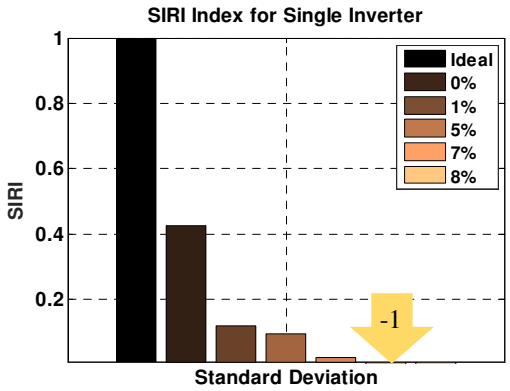

Fig. 5. SIRI index for a single grid-tied PV inverter system with different current sensing inaccuracies.

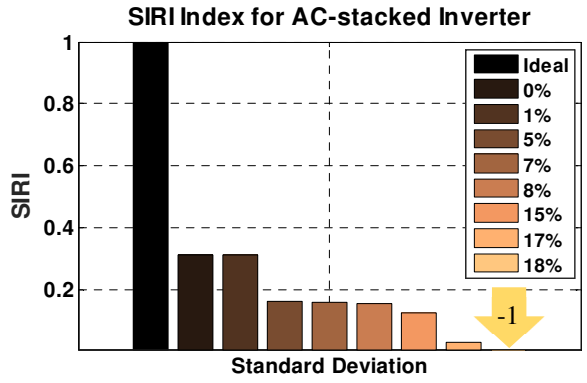

Fig. 6. SIRI index for an AC-stacked grid-tied PV inverter system with different current sensing inaccuracies.

V. Conclusion

This paper analyzed and evaluated the impact of current sensing inaccuracies on the robustness of grid-tied AC-stacked PV inverter systems. We utilized a novel comparative index for evaluating the robustness of modern smart PV inverters. The index not only determines the robustness

boundary for operation of PV inverters, it also comparatively evaluates the inverters in robust region that can be used as a tool for comparing different PV architectures. The focus of this paper was on comparative analysis between single inverter and AC-stacked inverter system. The study showed the AC-stacked inverter configuration due to its distributed control architecture, and using minimum measurement element units is more robust specially for current sensing inaccuracies. Moreover, by applying the Kalman filter algorithm as an estimation tool and enhancing the sensing signal accuracy, the robustness of the proposed PV inverters improved and the corresponding results presented.

ACKNOWLEDGEMENT

This work is supported by Electrical and Computer Engineering Department at University of North Carolina at Charlotte.

REFERENCES

[1] R. Renewable Energy Policy Network for thr 21st Centure, "Renewables and global status report 2016," 2016.

[2] M. Davoudi, V. Cecchi and J. R. Agüero, "Increasing penetration of Distributed Generation with meshed operation of distribution systems," 2014 North American Power Symposium (NAPS), Pullman, WA, 2014, pp. 1-6.

[3] Y. Yongheng, P. Enjeti, F. Blaabjerg, and W. Huai, "Suggested grid code modifications to ensure wide-scale adoption of photovoltaic energy in distributed power generation systems," in Industry Applications Society Annual Meeting, 2013 IEEE, 2013, pp. 1-8.

[4] M. Rashidi, A. Nasiri, R. Cuzner, "Application of Multi-Port Solid State Transformers for Microgrid-Based Distribution Systems", 2016 International Conference on Renewable Energy Research and Applications (ICRERA), Birmingham, UK, 2016,

[5] N. C. Sintamarean, F. Blaabjerg, H. Wang, F. Iannuzzo and P. de Place Rimmen, "Reliability Oriented Design Tool For the New Generation of Grid Connected PV-Inverters," in IEEE Transactions on Power Electronics, vol. 30, no. 5, pp. 2635-2644, May 2015.

[6] R. Teodorescu and M. Liserre, Grid Converters for Photovoltaic and Wind Power Systems. Wiley, 2011.

[7] A. Pigazo, M. Liserre, F. Blaabjerg and T. Kerekes, "Robustness analysis of the efficiency in PV inverters," IECON 2013 - 39th Annual Conference of the IEEE Industrial Electronics Society, Vienna, Austria, 2013, pp. 7015-7020.

[8] M. Biglarbegian, S. Nibir, H. Jafarian, J. Enslin, B. Parkhideh., "Layout Study of Contacless Magnetoresistor Current Sensor for High Frequency Converters," in IEEE Energy Conversion Congress and Exposition (ECCE), Milwaukee, 2016, In press.

[9] H. Jafarian, B. Parkhideh, and S. Bhowmik "Robustness Evaluation of Grid-tied AC-stacked PV Inverter System Considering Manufacturing Inaccuracies" 42nd Annual IEEE Conference of Industrial Electronics Society (IECON), Florence, 2016, (In press)

[10] M. Moosavi, S. Farhangi, H. Iman-Eini and A. Haddadi, "An LCL-based interface connecting photovoltaic back-up inverter to load and grid," 4th Annual International Power Electronics, Drive Systems and Technologies Conference, Tehran, 2013, pp. 465-470.

[11] D. Ricchiuto, M. Liserre, T. Kerekes, R. Teodorescu and F. Blaabjerg, "Robustness analysis of active damping methods for an inverter connected to the grid with an LCL-filter," 2011 IEEE Energy Conversion Congress and Exposition, Phoenix, AZ, 2011, pp. 2028-2035.

[12] H. Jafarian, B. Parkhideh and S. Bhowmik, "A novel comparative robustness index for evaluating the performance of grid-tied PV inverters," 2016 IEEE 43rd Photovoltaic Specialists Conference (PVSC), Portland, OR, USA, 2016, pp. 1254-1259.

[13] A. Kulkarni and V. John, "Mitigation of Lower Order Harmonics in a Grid-Connected Single-Phase PV Inverter," in IEEE Transactions on Power Electronics, vol. 28, no. 11, pp. 5024-5037, Nov. 2013.

[14] A. Marzoughi and H. Imaneini, "An optimal selective harmonic mitigation for cascaded H-bridge converters," 2012 11th International Conference on Environment and Electrical Engineering, Venice, 2012, pp. 752-757.

[15] Alinaghi Marzoughi, Hossein Imaneini, Amirhossein Moeini, An optimal selective harmonic mitigation technique for high power converters, International Journal of Electrical Power & Energy Systems, Volume 49, July 2013, Pages 34-39.

[16] M. Moosavi, G. Farivar, H. Iman-Eini and S. M. Shekarabi, "A voltage balancing strategy with extended operating region for cascaded H-bridge converters," in IEEE Transactions on Power Electronics, vol. 29, no. 9, pp. 5044-5053, Sept. 2014.

[17] Y. Yang, H. Wang and F. Blaabjerg, "Reactive Power Injection Strategies for Single-Phase Photovoltaic Systems Considering Grid Requirements," in IEEE Transactions on Industry Applications, vol. 50, no. 6, pp. 4065-4076, Nov.-Dec. 2014.

[18] L. Liu, H. Li, Y. Xue and W. Liu, "Reactive Power Compensation and Optimization Strategy for Grid-Interactive Cascaded Photovoltaic Systems," in IEEE Transactions on Power Electronics, vol. 30, no. 1, pp. 188-202, Jan. 2015.

[19] A. Cagnano, E. De Tuglie, M. Liserre and R. A. Mastromauro, "Online Optimal Reactive Power Control Strategy of PV Inverters," in IEEE Transactions on Industrial Electronics, vol. 58, no. 10, pp. 4549-4558, Oct. 2011.

[20] M. Jantsch et al., "Measurement of PV maximum power point tracking performance," in 14th European photovoltaic solar energy conference and exhibition, Barcelona, 1997.

[21] A. Driesse, S. Harrison and P. Jain, "Evaluating the Effectiveness of Maximum Power Point Tracking Methods in Photovoltaic Power Systems using Array Performance Models," 2007 IEEE Power Electronics Specialists Conference, Orlando, FL, 2007, pp. 145-151.

[22] G. Fishman, Monte Carlo Concepts, Algorithms, and Applications. Springer, 1996.

[23] M. Keramat and R. Kielbasa, "Modified Latin Hypercube Sampling Monte Carlo (MLHSMC) Estimation for Average Quality Index," Analog Integr. Circuits Signal Process., vol. 19, no. 1, pp. 87-98, 1999.

[24] H. Jafarian et al., "Design and implementation of distributed control architecture of an AC-stacked PV inverter," 2015 IEEE Energy Conversion Congress and Exposition (ECCE), Montreal, QC, 2015, pp. 1130-1135.

[25] F. Gustafsson, "Adaptive Filtering and Change Detection," Wiley, 2000.

[26] M. Biglarbegian, S. J. Nibir, H. Jafarian, and B. Parkhideh, "Development of current measurement techniques for high frequency power converters," in 2016 IEEE International Telecommunications Energy Conference (INTELEC), Austin, 2016, pp. 1-7.

[27] http://www.allegromicro.com/en/Products/Current-Sensor-ICs/Zero-To-Fifty-Amp-Integrated-Conductor-Sensor-ICs/ACS730.aspx

[28] http://www.allegromicro.com/en/Products/Current-Sensor-ICs/Zero-To-Fifty-Amp-Integrated-Conductor-Sensor-ICs/ACS714.aspx